

Weierstraß-Institut für Angewandte Analysis und Stochastik

im Forschungsverbund Berlin e.V.

Preprint

ISSN 0946 – 8633

Chaotic bound state of localized structures in the complex Ginzburg-Landau equation

Dmitry Turaev ¹, Andrei Vladimirov ²,

and Sergey Zelik ²

submitted: 17th July 2005

¹ Ben Gurion University
P.O.B. 653 84105 Be'er Sheva
Israel
E-Mail: turaev@math.bgu.ac.il

² Weierstrass Institute for Applied
Analysis and Stochastics,
Mohrenstrasse 39, D - 10117 Berlin
Germany
E-Mail: vladimir@wias-berlin.de
zelik@wias-berlin.de

No. 1152
Berlin 2006



2000 *Mathematics Subject Classification.* 78A60, 35Q60, 35B32.

Key words and phrases. dissipative soliton, pulse interaction, homoclinic bifurcation.

1999 *Physics and Astronomy Classification Scheme.* 42.65.Sf, 05.45.-a, 42.65.Tg.

Edited by
Weierstraß-Institut für Angewandte Analysis und Stochastik (WIAS)
Mohrenstraße 39
10117 Berlin
Germany

Fax: + 49 30 2044975
E-Mail: preprint@wias-berlin.de
World Wide Web: <http://www.wias-berlin.de/>

Abstract

A new type of stable dynamic bound state of dissipative localized structures is found. It is characterized by chaotic oscillations of distance between the localized structures, their phase difference, and the center of mass velocity.

Complex Ginzburg-Landau equation describes the onset of instability near a Hopf bifurcation in spatially extended systems and, therefore, serves as a universal model for various physical phenomena in hydrodynamics, superconductivity and optics. In a certain parameter range this equation exhibits a spatially localized solution — a dissipative soliton. In the classical setting with purely cubic nonlinearity, the soliton is unstable. In order to describe stable dissipative solitons, the next order nonlinear terms should be taken into account [1]. Thus, the quintic complex Ginzburg-Landau equation (QCGLE) is widely used in nonlinear optics to describe different phenomena related to pulse formation, such as mode-locking in lasers [2, 7], light propagation in nonlinear fibers [3], transverse pattern formation in nonlinear optical systems [4]. In particular, in mode-locked fiber lasers dissipative solitons appear as short optical pulses propagating along the cavity axis. Being well separated from one another, the pulses interact via their exponentially decaying tails. Interference between the tails can produce spatial intensity oscillations responsible for the formation of bound states of the dissipative solitons (see e.g. experimental studies in Refs. [5, 6, 7]). Up to now, either stationary and uniformly moving [8, 9, 10], or uniformly rotating [11] bound states were reported. Here we show that slight breaking the phase-shift symmetry can produce a huge variety of dynamic bound states, characterized by undamped oscillations, regular or chaotic ones, of the solitons coordinates and phases.

It is typical of the weak interaction of dissipative solitons that the shape of the solitons in the bound state is preserved, while their positions and certain internal parameters, such as phases, evolve slowly with time. Gorshkov-Ostrovsky approach [13, 14] allows one to derive a set of finite dimensional soliton interaction equations (SIE) that govern the slow evolution of the soliton parameters. Being independent of the specific details of a concrete model, the form of SIE is largely determined by the asymptotical behavior of the soliton tails and by the symmetries of the model. In particular, when the model admits only translational symmetry, SIE have a gradient structure (see e.g. Ref. [14]), which implies a trivial dynamics for the weakly interacting solitons (only stationary or uniformly moving bound states). In the case of QCGLE, the additional phase-shift symmetry changes the structure of SIE. However, the dynamics of the weak two-soliton interaction still remains simple and the only attractors are bound states characterized by time independent

distance and phase difference between the solitons [9, 10]. Thus, one might expect that the breakdown of the phase-shift symmetry would make the dynamics only simpler. On the contrary, as we show here, breaking the phase-shift symmetry leads to the explosion of the complexity of the two-soliton interaction dynamics (the gradient structure restores only at relatively large values of the symmetry breaking parameter). Note that the localized in space and chaotic in time regimes which we discover are very different from the earlier known ones, for whom the chaos was a feature of the internal dynamics of a single soliton [12] or was related to a scattering process with unbounded soliton trajectories [15]. In our case, chaos is associated with a strange attractor that forms solely due to the weak soliton interaction.

We consider 1+1 dimensional QCGLE in the form

$$\partial_t A = (\beta + i/2)\partial_{xx}A + A [\delta + (\varepsilon + i)|A|^2 + (\mu + i\nu)|A|^4] + \eta \exp(i\Omega t), \quad (1)$$

with complex amplitude $A(x, t)$. Equation (1) is symmetric with respect to spatial translations, and it also possesses the phase-shift symmetry $A \rightarrow A \exp(i\chi)$ at $\eta = 0$. The meaning of the parameters (all real) is the following: $\beta > 0$ is the diffusion coefficient (the second order dispersion is scaled to 1/2), $\delta > 0$ describes linear losses; ε , μ and ν define the shape of nonlinearity. An important application concerns with Kerr-lens mode-locked laser [7]. Then, A is a normalized electromagnetic field envelope, and the symmetry breaking term $\eta \exp(i\Omega t)$ corresponds to a weak signal injected into the laser.

Assume α to be the frequency shift of a single soliton solution at $\eta = 0$. Then this solution takes the form $A = A_0(x) \exp(i\alpha t)$. Away from the soliton core, $A_0(x)$ decays exponentially:

$$A_0(x) \sim p \exp [(-\gamma + i\omega)|x|] \quad \text{as } |x| \rightarrow \infty. \quad (2)$$

The stability of the soliton is determined by the spectrum of the operator L_0 obtained by the linearization of the right hand side of Eq. (1) on the soliton at $\eta = 0$. Note that L_0 has two neutral modes, $\Psi(x) = iA_0(x)$ and $\Sigma(x) = \partial_x A_0(x)$, corresponding, respectively, to the phase-shift and translational symmetries of the unperturbed QCGLE. It follows that the adjoint operator L_0^\dagger has two neutral modes too, $\Psi^\dagger(x)$ and $\Sigma^\dagger(x)$. We fix their choice by the normalization conditions $\int_{-\infty}^{\infty} \Psi^\dagger \Psi dx = 1$ and $\int_{-\infty}^{\infty} \Sigma^\dagger \Sigma dx = 1$. Note that

$$\begin{aligned} \Psi^\dagger(x) &\sim q \exp [(-\gamma + i\omega)|x|], \\ \Sigma^\dagger(x) &\sim s \exp [(-\gamma + i\omega)|x|], \end{aligned} \quad (3)$$

as $|x| \rightarrow \infty$, with certain complex constants q and s .

Up to the leading order in $\exp(-\gamma r)$ (where r is the distance between the solitons), a bound state of two weakly interacting solitons has the form

$$A = \exp(i\alpha t) \left[A_0(x - x_1) e^{i\varphi_1} + A_0(x - x_2) e^{i\varphi_2} \right], \quad (4)$$

where the coordinates $x_{1,2}$ and phases $\varphi_{1,2}$ of the individual solitons are slowly varying functions of time t . By plugging this ansatz into Eq. (1) and projecting the

resulting equations onto the tangent to the space of functions of type (4), we obtain the following SIE:

$$\partial_t r = a \exp(-\gamma r) \sin(\omega r + \theta_1) \cos \varphi, \quad (5)$$

$$\partial_t \varphi = -b \exp(-\gamma r) \cos(\omega r + \theta_2) \sin \varphi - c \eta \sin \frac{\varphi}{2} \sin \frac{\Phi}{2}, \quad (6)$$

$$\partial_t \Phi = b \exp(-\gamma r) \sin(\omega r + \theta_2) \cos \varphi + c \eta \cos \frac{\varphi}{2} \cos \frac{\Phi}{2} + 2\Delta, \quad (7)$$

$$V = -a \exp(-\gamma r) \cos(\omega r + \theta_1) \sin \varphi, \quad (8)$$

where $r = x_2 - x_1$, $\varphi = \varphi_2 - \varphi_1$, $\Phi = \varphi_1 + \varphi_2 - 2\zeta$, and $V = \partial_t(x_1 + x_2)/2$. The parameter $\Delta = \Omega - \alpha$ describes the frequency detuning between the injected field and the single soliton solution. The other parameters are defined by $a \exp(i\theta_1) = 4pq [-(\gamma - 2\beta\omega) + i(\omega + 2\beta\gamma)]$, $b \exp(i\theta_2) = 4ps [(\gamma - 2\beta\omega) - i(\omega + 2\beta\gamma)]$, and $c \exp(i\zeta) = 4 \int_{-\infty}^{\infty} \Psi^\dagger dx$, where p, q, s are the coefficients of asymptotics (2) and (3).

For more details on the derivation of the SIE see Ref. [10]. Being obtained formally, using a multiscale method, system (5)-(8) needs a justification. The strongest one is given by the ‘‘invariant manifold theorem’’ of Ref. [16]. It is a general statement which holds for all multisoliton weak interaction processes in a large class of PDE’s under the condition of a non-zero diffusion. In our case, for $\beta \neq 0$, the theorem ensures the existence of a closed set of four ODE’s (‘‘the true SIE’’) which give an exact description of the weak interaction of two solitons, valid uniformly on unbounded time intervals. Moreover, it follows from the proof, that the formal scheme employed in the derivation of Eqs. (5)-(8) yields an $o[\exp(-\gamma r)]$ -approximation to the true SIE. Note the importance of the non-zero diffusion. For example, for conservative systems the long-time validity of SIE must be questioned.

First, we consider Eqs. (5)-(8) with $\eta = 0$. The system then retains the phase-shift symmetry, so Eq. (7) for the sum of the soliton phases Φ decouples from the other equations. Thus, in this case the dynamics of the soliton interaction is described by the two-dimensional system

$$\begin{aligned} \partial_t r &= a \exp(-\gamma r) \sin(\omega r + \theta_1) \cos \varphi, \\ \partial_t \varphi &= -b \exp(-\gamma r) \cos(\omega r + \theta_2) \sin \varphi. \end{aligned} \quad (9)$$

This system is reversible, i.e. invariant under the transformation $t \rightarrow -t$, $\varphi \rightarrow \pi - \varphi$. As usual in dimension two, the reversibility implies integrability. The integral is $H = \sin \varphi \exp[-br \sin(\theta_2 - \theta_1)/a] |\sin(\omega r + \theta_1)|^{b \cos(\theta_2 - \theta_1)/(a\omega)}$. The trajectories of (9) comprise the level lines of H , so the phase portrait of (9) can easily be recovered. Two types of phase portraits are possible [10] depending on the sign of $\rho = ab\omega \cos(\theta_2 - \theta_1)$. Here we consider only the case $\rho > 0$ when the phase trajectories are closed curves surrounding the neutrally stable equilibria $S_{k\pm\pi/2} : \{\varphi = \pm\pi/2, \omega r + \theta_2 = \pi(k + 1/2)\}$, see Fig. 1a. It follows from Eq. (8) that the $\pm\pi/2$ -out-of-phase equilibria correspond to uniformly moving bound soliton states. Two other sets of equilibria, the saddle ones, correspond to stationary bound states, in-phase $S_{k0} : \{\varphi = 0, \omega r + \theta_2 = 2\pi k\}$ and anti-phase $S_{k\pi} : \{\varphi = \pi, \omega r + \theta_2 =$

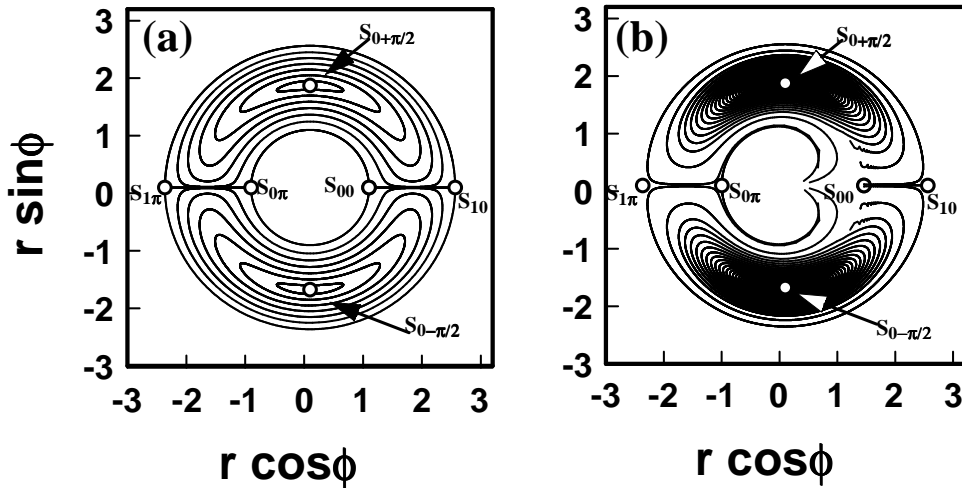


Figure 1: Phase portraits obtained by numerical solution of (a) the SIE (9) and (b) the QCGLE (1) at $\eta = 0$. The parameters here and in the following Figures are: $\beta = 0.5$, $\delta = 0.02$, $\varepsilon = 1.8$, $\mu = 0.05$, $\nu = 0.05$. This corresponds to $\omega = -2.149$, $\gamma = 5.195$, $a = 0.118$, $b = 7.55 \cdot 10^{-4}$, $\theta_1 = 6.82 \cdot 10^{-4}$, $\theta_2 = 2.25$ in the SIE.

$\pi(2k + 1)\}$. The separatrices of the saddles divide the phase plane into cells, from which the trajectories can never escape, see Fig. 1a.

Recall that Eqs. (9) are an approximation of a certain true SIE. In fact, the higher order corrections destroy the reversibility, and hence the integrability, of the SIE. Indeed, it is seen from Fig. 1b where the results of a direct simulation of Eq. (1) are presented (cf. Ref. [9]), that rather than being closed, trajectories slowly spiral towards the weakly stable $\pm\pi/2$ -out-of-phase equilibria. Furthermore, the cells boundaries break: a trajectory can flow from cell to cell until it is captured to one of the $\pm\pi/2$ -out-of-phase bound states, or leaves the weak interaction zone — then the two-soliton state collapses to a single soliton.

When $\eta \neq 0$, Eq. (7) couples with Eqs. (5) and (6). The dynamics is then determined by the ratios between η , Δ , and $\exp(-\gamma r)$. Let us show that chaos should be expected when $\Delta \gg \eta, \exp(-\gamma r)$. Indeed, as the sum of the soliton phases Φ rotates with nonzero velocity in this case, Φ can be taken as a new time variable. Thus, system (5)-(7) is, effectively, a periodic perturbation of the conservative integrable system (9). Such systems do exhibit a chaotic behavior due to the destruction of resonances. So, near every resonance zone, i.e. in the vicinity of those periodic trajectories of Eqs. (9) for which the increment of Φ during the period is commensurate with 4π , the soliton interaction dynamics can be chaotic. Since the higher order corrections introduce a weak dissipation into the SIE, most of the resonances are, in fact, erased. However, as we will see below, the chaotic dynamics produced by the strongest resonances can survive.

One more possibility for chaos is the splitting of the cell boundaries. As the phase Φ rotates, the in-phase and anti-phase equilibria of Eqs. (9) become saddle peri-

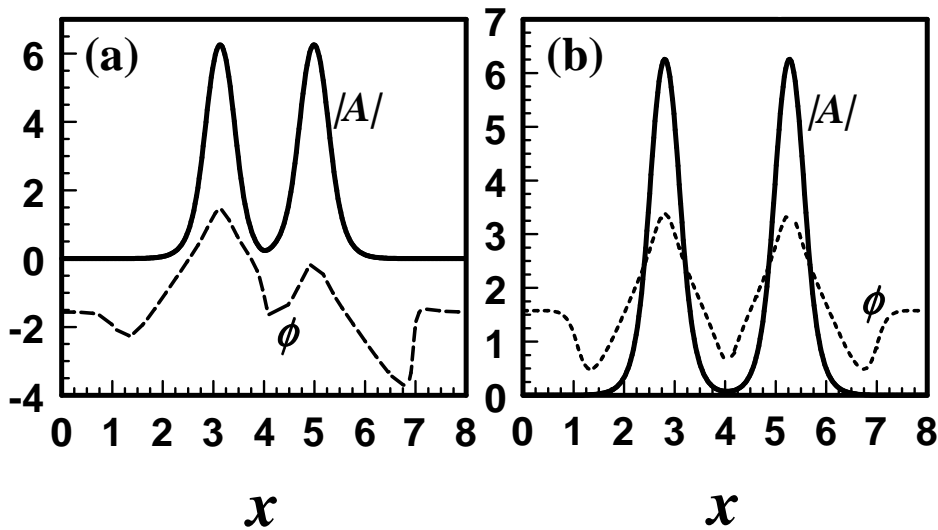


Figure 2: Stable bound states with the phase difference $\phi = \pi/2$ (a) and $\phi = 0$ (b) between the solitons.

odic orbits of Eqs. (5)-(7) at $\eta \neq 0$, and their stable and unstable manifolds may intersect. Thus, zones of a “metastable” homoclinic chaos can be formed. This type of behavior is characterized by large oscillations in phase difference ϕ , i.e. we see chaotic transitions between the cells in the (r, ϕ) -plane (Fig. 5g).

It is noteworthy that the spatial motion of chaotic bound states is, effectively, a random walk at large time scales: as Eq. (8) shows, when the dynamics of r and φ is chaotic, the center of mass velocity V is a random function of time (with a certain non-zero decay of correlation time), so the spatial position of the chaotic bound state is an integral of a random signal.

Another, nonrotational mechanism of chaos creation in the SIE is related to multiple bifurcations of equilibrium states. As we mentioned, the equilibria of Eqs. (9) correspond, in general, to periodic orbits of Eqs. (5)-(7). However, at moderate values of Δ/η , due to a synchronization phenomenon, bound states with stationary r , φ_1 , and φ_2 can form (see Fig. 2). The stability domains for the $\pm\pi/2$ -out-of-phase and in-phase equilibria of Eqs. (5)-(7) are shown in Figs. 3a and 3b, respectively. The birth of $\pm\pi/2$ -out-of-phase equilibria is accompanied here by a simultaneous Andronov-Hopf bifurcation, i.e. in addition to a zero characteristic eigenvalue these equilibria have a pair of pure imaginary eigenvalues. Such double bifurcation is known (see Ref. [17]) to lead to a chaotic behavior via a Shilnikov homoclinic loop. Another multiple instability, also leading to Shilnikov chaos [18], corresponds to a triplet of zero characteristic eigenvalues of the $\pm\pi/2$ -out-of-phase equilibrium at $|\Delta| = c|\eta|/\sqrt{8} = (\sqrt{\rho + b^2/4} \pm b/2) \exp\{-\gamma[\pi(k + 1/2) - \theta_2]/\omega\}$. Although higher order corrections to SIE (5)-(7) cause a decrease in the multiplicity of the local bifurcations, the chaos associated with them has to persist nevertheless.

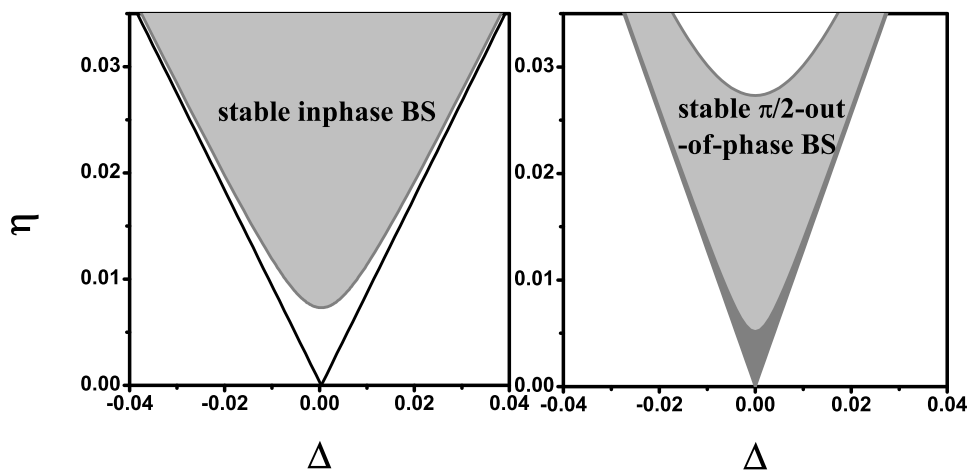


Figure 3: Stability domains (grey) of the $\pi/2$ -out-of-phase and in-phase bound soliton states on the (η, Δ) parameter plane.

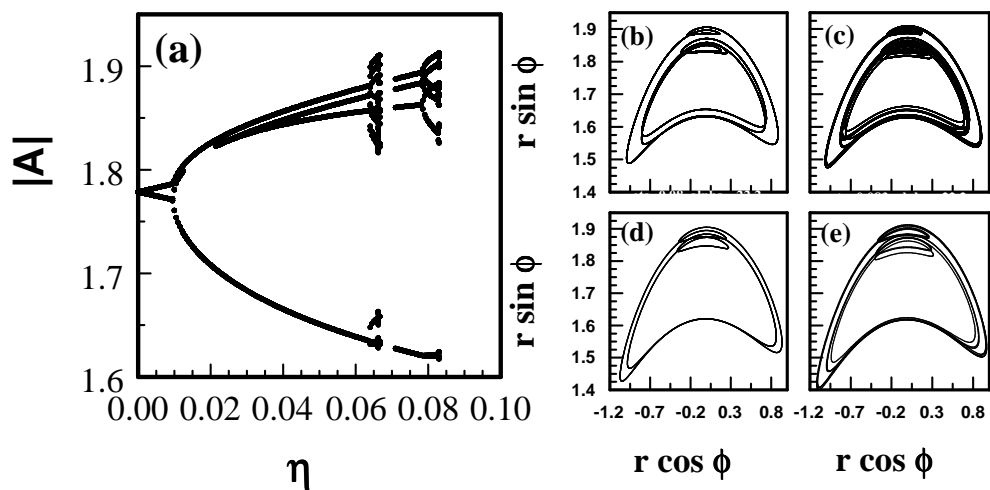


Figure 4: Simulation results for the QCGLE. (a) – bifurcation tree calculated for $\Omega = -22.2$. (b) – period three, $\eta = 0.065$; (c) – chaotic, $\eta = 0.06623$; (d) – period two, $\eta = 0.08$; and (e) – period six, $\eta = 0.083$, soliton bound states.

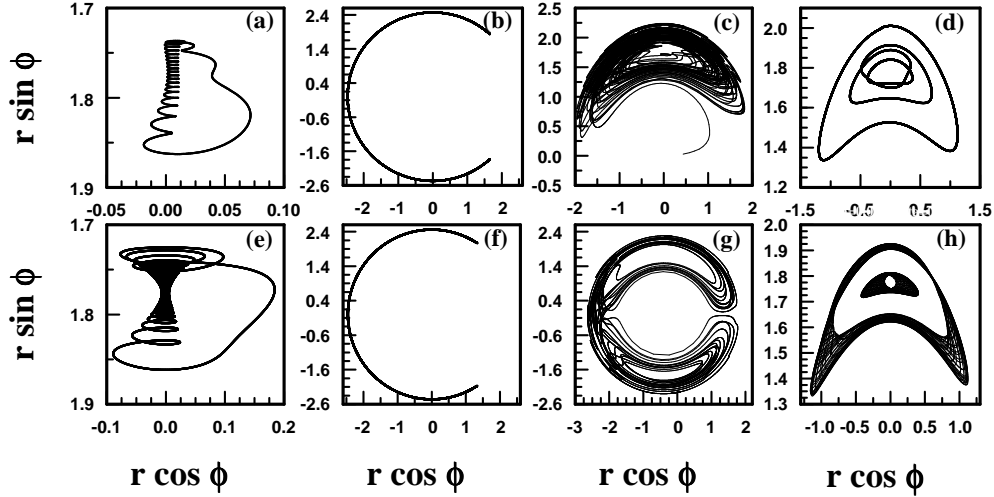


Figure 5: Phase portraits obtained by solving numerically the QCGLE (a)-(d) and SIE (e)-(h). (a) $\eta = 0.02$, $\Omega = -22.3465$, (b) $\eta = 0.4$, $\Omega = -22.2$, (c) $\eta = 0.06$, $\Omega = -22.2$, (d) $\eta = 0.02$, $\Omega = -22.25$, (e) $\eta = 0.02$, $\Delta = -0.0164$, (f) $\eta = 0.02$, $\Delta = 0.023$, (g) $\eta = 0.02$, $\Delta = 0.11$, (h) $\eta = 0.11$, $\Delta = 0.41$.

The above analysis is pretty much confirmed by the results of a direct simulation of Eq. (1). Fig. 4(a) shows the evolution (the “bifurcation tree”) for the $\pi/2$ -out-of-phase regime with the change of the injected signal amplitude η . Away from the synchronization range, the regime undergoes a number of period-doubling and period-tripling bifurcations (strong 1:2 and 1:3 resonances) leading, in particular, to chaotic behavior [a “strange attractor”, see Fig. 4(b)]. Different other dynamical regimes are shown in Fig. 5 where the phase portraits in the upper row are obtained by numerical solution of Eq. (1), while those in the lower row correspond to Eqs. (5)-(7). Figures 5(a) and 5(e) illustrate a desynchronization transition from the stationary $\pi/2$ -out-of-phase bound state to a stable limit cycle via a homoclinic bifurcation (cf. Ref. [19]). A stable limit cycle born from a homoclinic loop to a saddle anti-phase state is shown in Figs. 5(b) and 5(f). Figure 5(c) shows a metastable chaotic bound state which corresponds to a stable chaotic regime of Eqs. (5)-(7) [see Fig. 5(g)]. Finally, Fig. 5(d) illustrates multistability between different time-periodic bound states of Eq. (1). The corresponding quasiperiodic solutions of Eqs. (5)-(7) are shown in Fig. 5(h). The comparison of the phase portraits in the upper and lower rows in Fig. 5 reveals a substantial similarity between the solutions of Eq. (1) and those of Eqs. (5)-(7). There is no one-to-one correspondence, however, because in Eqs. (5)-(7) we have neglected second and higher order terms in $\exp(-\gamma r)$ that are responsible for a weak dissipation. Though these terms are small, they are not negligible in the first two elementary cells of the phase space that are depicted in Fig. 1a. In the next cells that correspond to larger soliton separations one should expect a similar behavior, though with much weaker dissipation effects.

As we see, the weak interaction of two dissipative solitons can produce a very rich

dynamics. The mechanism of a creation of dynamic (e.g. chaotic) soliton bound states is related to the breakdown of the phase-shift symmetry and has a universal, model-independent nature. Therefore, it should be typical for every spatially extended system which undergoes a Hopf bifurcation. In particular, in laser systems, violation of the phase-shift symmetry can be straightforwardly achieved by an injection of an external signal, so the effects described in this letter can be a subject of experimental observations. The fact that the two-soliton state in the QCGLE is a weakly damped nonlinear oscillator can be used to analyze the dynamics of soliton bound states in other situations. Thus, a system of 4 interacting solitons can be viewed as a pair of coupled, weakly damped oscillators, i.e. it has to produce a rich dynamical behavior even without the phase-shift symmetry breaking. Similar effects should be expected for the case of rotating soliton bound states in two space dimensions.

This work was supported by grants Terabit Optics Berlin 10017606 and ISF 926/04.

References

- [1] O. Thual and S. Fauve, *J. Phys. (France)* **49**, 1829 (1988).
- [2] J.D. Moores, *Optics Communications* **96**, 65 (1993).
- [3] N.N. Akhmediev and A. Ankiewicz, *Solitons. Nonlinear Pulses and Beams* (Chapman and Hall, London, 1997).
- [4] P. Mandel and M. Tlidi, *J. Opt. B* **6**, R60 (2004).
- [5] D.Y. Tang *et al.*, *Phys. Rev. A* **64**, 033814 (2001); **68**, 013816 (2003).
- [6] P. Grelu *et al.*, *Opt. Lett.* **27**, 966 (2002); *Opt. Express* **11**, 2238 (2003).
- [7] P. Grelu and N. Akhmediev, *Opt. Express* **12**, 3184 (2004).
- [8] H.R. Brand and R. J. Deissler, *Phys. Rev. Lett.* **63**, 2801 (1989); B.A. Malomed, *Phys. Rev. A* **44**, 6954 (1991); V.V. Afanasjev and N. Akhmediev, *Phys. Rev. E* **53**, 6471 (1996).
- [9] N.N. Akhmediev, A. Ankiewicz, and J.M. Soto-Crespo, *Phys. Rev. Lett.* **79**, 4047 (1997).
- [10] A.G. Vladimirov, G.V. Khodova, and N.N. Rosanov, *Phys. Rev. E* **63**, 056607 (2001).
- [11] D.V Skryabin and A.G. Vladimirov, *Phys. Rev. Lett.* **89**, 044101 (2002); N.N. Rosanov, S.V. Fedorov, and A.N. Shatsev, *Phys. Rev. Lett.* **95**, 053903 (2005).
- [12] J.M. Soto-Crespo, N. Akhmediev, and A. Ankiewicz, *Phys. Rev. Lett.* **85**, 2937 (2000).

- [13] K.A. Gorshkov, L.A. Ostrovsky, and V.V. Papko, *Sov. Phys. JETP* **44**, 306 (1976); K.A. Gorshkov and L.A. Ostrovsky, *Physica* **3D**, 428 (1981).
- [14] I.S. Aranson *et al.*, *Physica* **43D**, 435 (1990).
- [15] K.A. Gorshkov, A.S. Lomov, and M.I. Rabinovich, *Nonlinearity* **5**, 1343 (1992).
- [16] B.Sandstede, in *Handbook of Dynamical Systems II*, edited by B. Fiedler (Elsevier, Amsterdam, 2002); S. Zelik and A. Mielke, WIAS Berlin, Preprint No. 1093, 2006.
- [17] J. Guckenheimer and P. Holmes, *Nonlinear Oscillations, Dynamical Systems, and Bifurcations of Vector Fields* (Springer, 1983).
- [18] A. Arneodo *et al.*, *Physica* **14D**, 327 (1985); S. Ibáñez and J.A. Rodríguez, *J. Diff. Equ.* **208**, 147 (2005).
- [19] N.K. Gavrilov and A.L. Shilnikov, *Amer. Math. Soc. Transl.* **200**, 165 (2000); B. Krauskopf and S. Wiczorek, *Physica* **173D**, 114 (2002).